

Review

A Review of the Performance Improvement Methods of Phase Change Materials: Application for the Heat Pump Heating System

Cong Zhou ^{1,2,†}, Yizhen Li ^{2,*,†}, Fenghao Wang ^{2,*}, Zeyuan Wang ², Qing Xia ², Yuping Zhang ³, Jun Liu ³, Boyang Liu ¹ and Wanlong Cai ² 

¹ Shannxi Zhongmei New Energy Co., Ltd., Xi'an 710054, China

² School of Human Settlements and Civil Engineering, Xi'an Jiaotong University, Xi'an 710049, China

³ Key Laboratory of Coal Resources Exploration and Comprehensive Utilization, Ministry of Natural Resources, Xi'an 710021, China

* Correspondence: lyz0503@stu.xjtu.edu.cn (Y.L.); fhwang@mail.xjtu.edu.cn (F.W.)

† These authors contributed equally to this work.

Abstract: With the development of the economy and society, energy problems have become a great concern. The heat pump-coupled thermal energy storage (TES) system is a potential form of building heating, which can improve the stability of the grid and promote the consumption of renewable energy. Phase change materials (PCMs) are widely used in the field of building heating, but there are still some problems such as unsatisfactory melting points, low thermal conductivity, phase separation, and supercooling, which limit the application of PCMs in heat pump heating systems. Therefore, it is very important to improve PCMs by a performance improvement method. This work first summarizes the classification, advantages and disadvantages of PCMs, and introduces the connection between PCMs and heat pumps. Then, a detailed summary of PCMs applied in heat pump heating systems is presented, and a comprehensive review of the performance improvement methods for PCMs, which include additives, encapsulation, and eutectic compounds, is discussed. Finally, the existing problems, solutions, and future research directions are proposed. The emphasis of the research is to clarify the influence of PCMs on heat pump performance and the effect of different performance improvement methods on PCMs, and to illustrate the future development direction for PCMs in heat pump heating technologies, including the matching of heat pumps and PCMs, multi-standard decision methods and advanced control strategies.

Keywords: thermal energy storage; phase change materials; heat pump heating system; performance improvement methods



Citation: Zhou, C.; Li, Y.; Wang, F.; Wang, Z.; Xia, Q.; Zhang, Y.; Liu, J.; Liu, B.; Cai, W. A Review of the Performance Improvement Methods of Phase Change Materials: Application for the Heat Pump Heating System. *Energies* **2023**, *16*, 2676. <https://doi.org/10.3390/en16062676>

Academic Editors: Fabio Polonara, Sandro Nizetic, Vitor António Ferreira da Costa and Alice Mugnini

Received: 21 January 2023

Revised: 4 March 2023

Accepted: 6 March 2023

Published: 13 March 2023



Copyright: © 2023 by the authors. Licensee MDPI, Basel, Switzerland. This article is an open access article distributed under the terms and conditions of the Creative Commons Attribution (CC BY) license (<https://creativecommons.org/licenses/by/4.0/>).

1. Introduction

With the rapid development of the economy and society worldwide, people are increasingly concerned about the problem of global warming. Countries have passed legislation setting ambitious climate and energy targets in pursuing carbon neutrality by 2050 or sooner [1]. One of the important drivers of climate change is the increase in the level of greenhouse gases (GHG) in the atmosphere, which is mainly generated by the use of fossil energy; therefore, it is crucial to achieve the energy transition (ET) from fossil to renewable energy systems [2]. Building energy consumption accounts for a significant portion of both total energy consumption and carbon emissions, especially for the heating of buildings [3]. Making full use of renewable energy is an important solution for energy saving and emission reduction in buildings, and the heat pump (HP) is necessary to achieve this solution [4]. The heat pump is an energy-saving device that makes full use of renewable energy sources, usually by obtaining heat energy from the air, water, shallow soil, or medium-deep soil [5], doing work with electricity, and then providing heat

energy that far exceeds its electrical consumption. Heat pumps can replace combustion equipment and electric heating equipment in buildings, using renewable energy to develop the decarbonized economy. However, there are certain limitations in the application of heat pumps, such as frost accumulation on the surface of outdoor heat exchangers for air-source heat pumps (ASHPs) [6] and the imbalance of soil temperature for ground-source heat pumps (GSHPs) [7].

When using heat pumps to heat buildings, the operation of heat pumps requires a large amount of electricity, which often puts tremendous pressure on the power grid and results in a grid imbalance [8]. Thermal energy storage (TES) is an important technology to improve grid flexibility and renewable energy utilization, it stores electricity in the form of thermal energy in storage tanks during low peak hours and releases the stored heat to users during peak hours, thus reducing peak electricity consumption and balancing grid fluctuations [9]. Considering the operational characteristics of heat pumps and the peak cut effect of TES, coupling a heat pump heating system with a TES system can effectively improve the performance of heat pumps, such as shortening the defrosting time of air-source heat pumps [10], as well as performing power demand response (DR) to achieve real-time interactions with the grid, enhancing grid stability and system economy through demand-side management (DSM) [11], which has good potential for development.

The core of an energy storage system is the energy storage material. TES is divided into three types according to the heat storage mode, sensible heat storage, latent heat storage, and thermochemical heat storage. Among them, latent heat storage uses the large amount of latent heat generated by phase change materials (PCMs) during the phase change process to achieve heat storage and release, which can provide greater energy density and is widely used in building heating. As shown in Figure 1, PCMs are classified into organic, inorganic, and eutectic materials according to their material properties.

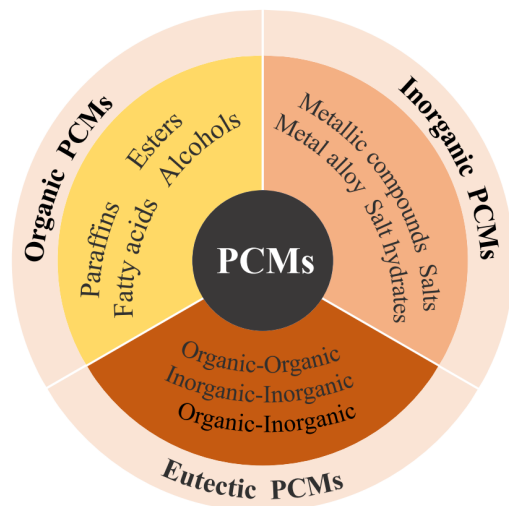


Figure 1. The different classifications of PCMs.

Table 1 compares the advantages and disadvantages of different types of PCMs [12,13]. Organic PCMs have good thermal and chemical stability, but low thermal conductivity; inorganic PCMs have large phase change enthalpy, but suffer from supercooling and phase separation; eutectic PCMs have good thermal physical properties, but there is a lack of currently available test data on their thermal physical properties. In heat pump heating systems, the thermal physical parameters of PCMs are carefully considered, including phase change temperature, thermal conductivity, and enthalpy of phase change, as they affect the overall performance of the heat pump heating system [14], and thus it is very important to enhance the properties and change the parameters of the materials through various techniques.

Table 1. The advantages and disadvantages of PCMs [12,13].

Type of PCMs	Advantages	Disadvantages
Organic PCMs	No supercooling No phase segregation Chemically stable Availability in large temperature range Compatibility with other materials Low vapor pressure	Low thermal conductivity Flammability Low phase change enthalpy More expensive Low heat capacity High volumetric expansion
Inorganic PCMs	High thermal conductivity Greater phase change enthalpy Less costly Lower volumetric expansion Compatibility with other materials Non-flammable	High supercooling Phase segregation Corrosive Chemical instability Low heat capacity
Eutectic PCMs	Sharp melting temperature High volumetric thermal storage density No phase segregation Low supercooling	Lack of thermophysical properties Low total latent heat capacity Costly

Many researchers have reviewed heat pump systems with TES [15,16] and improvement methods for PCMs [17,18]. Searching for previous reviews, as we know, there is just a limited comprehensive review of PCM materials deployed in heat pump heating systems and corresponding performance improvement techniques. In this paper, we provide a review of PCMs applied to heat pump heating systems, illustrate the link between heat pumps and PCMs, and provide a comprehensive discussion of material improvement techniques for heat pump heating in specific temperature ranges. This review provides theoretical guidance for the efficient design and practical application of heat pumps combined with TES systems.

2. PCMs and Heat Pumps

The main components of a heat pump usually include an evaporator, condenser, compressor, and expansion valve. Low-temperature and low-pressure vapour enters the compressor, then it is converted into vapour with high pressure and temperature. Afterwards, the vapour enters the condenser to release heat, and the incoming vapour is completely converted into a liquid. Subsequently, the liquid passes through the expansion valve, and its temperature and pressure drop, and this process makes the refrigerant a low-temperature and low-pressure liquid. After this, the liquid takes heat from the low-temperature heat source of the evaporator and turns it into vapour again. A diagram of the cycle is shown in Figure 2.

The theoretical coefficient of performance (COP) of heat pumps can be defined as the following Equation [19]:

$$COP = \frac{T_c}{T_c - T_v} = \frac{T_m + \Delta T_c}{T_m + \Delta T_c - (T_{amb} - \Delta T_v)} = \frac{T_m + \Delta T_c}{T_m - T_{amb} + (\Delta T_c + \Delta T_v)} \quad (1)$$

where T_c is the condensing temperature, T_v is the evaporating temperature, T_m is the temperature of the heat transfer medium of the condenser, ΔT_c is the temperature difference between the condenser and the heat transfer medium, T_{amb} is the temperature of the heat source, and ΔT_v is the temperature difference between the evaporator and the heat source. Assuming that ΔT_v is constant, COP will increase as ΔT_c decreases.

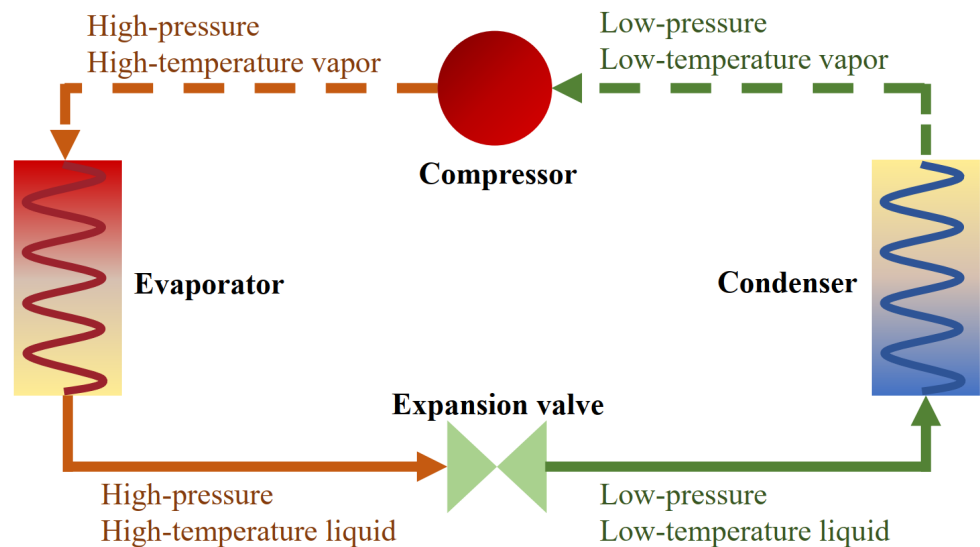


Figure 2. Working cycle of a heat pump.

Combining heat pumps and PCMs has three main advantages: firstly, PCMs can be combined with the condenser. As shown in Figure 3, after absorbing a large amount of heat, PCMs can undergo phase change in a small temperature range, which can maintain a relatively small temperature difference between the heat transfer medium and the condenser, thus improving the COP of the heat pump. Secondly, solar radiation is random and the air temperature varies greatly in cold climates, the thermal energy stored in PCMs can be used as a heat source for the evaporator, providing a stable evaporation temperature and facilitating the operation of the heat pump under stable conditions [20]. In addition, PCMs can solve the frost problem of ASHPs. When an ASHP runs in the winter under low external ambient temperatures, frost will appear on the outdoor coil. Due to the low thermal conductivity of frost, the performance of an ASHP decreases sharply and may even shut down [21]. To address this problem, the main defrosting methods include reverse-cycle defrosting and hot-gas bypass defrosting. The biggest problem of these two methods is the long defrosting time because there is no heat source in the defrosting cycle. In recent years, much attention has been paid to solving the frosting problem using heat exchangers with phase change materials [22].

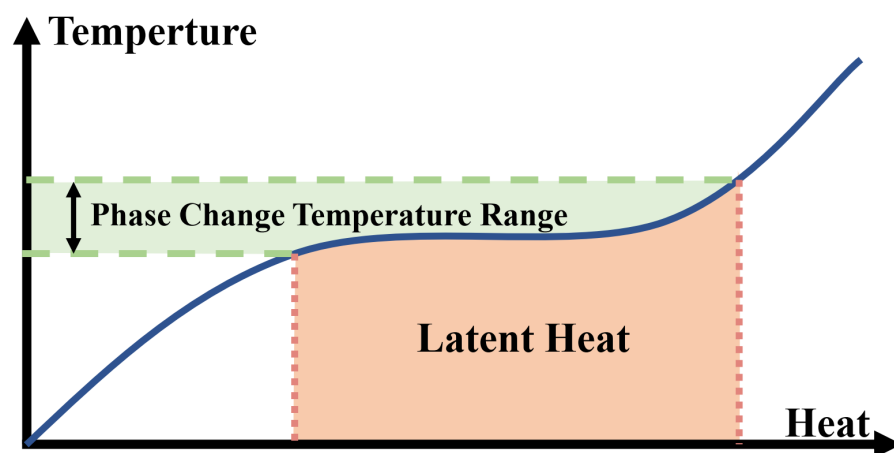


Figure 3. Phase change principle of PCMs.

For different types of heat pumps and application scenarios, a concise summary of PCMs coupled to heat pumps is presented in Table 2, and the thermophysical properties of these materials are labelled. While most studies are based on materials with different

melting points, such as sodium acetate trihydrate (SAT), calcium chloride hexahydrate, and paraffin, these PCMs, when applied to heat pump heating systems, exhibit relatively low latent heat and thermal conductivity. For heat pump heating systems, the melting point of PCMs is the first thing to consider. In the heat storage process, the inlet temperature of the storage tank needs to be higher than the melting point in order to make the complete phase change of the PCMs, the relatively high melting point of PCMs will prolong the time required for the complete phase change and reduce the efficiency of the heat pump heating system. In addition, the different temperature of the heating terminal will also affect the determination of the melting point. According to Table 2, PCMs with a melting temperature range of 40–60 °C are more suitable for space heating and domestic hot water supply. Thermal conductivity and thermal stability are also factors that must be considered. Low thermal conductivity of a PCM decreases the rate of heat storage and extraction [23], and reduces the heat transfer efficiency between the heat transfer fluid (HTF) and the PCM, seriously impacting the heat storage and release time of the TES system [21]. The thermal stability is related to the life cycle of the energy storage material and affects the operation of the whole energy storage system.

Table 2. Summary of PCMs applied to an HP.

Ref.	PCMs	T_m (°C)	ΔH_m (kJ/kg)	λ (W/(m·K))	Functions
[24]	Paraffin	56.03	254.9	-	Combined with condenser
[25]	RT58	51–63	-	-	Combined with condenser
[26]	Hydrated salt	48	210	0.45	Combined with condenser
[27]	SAT	47.8	219.8	-	Combined with condenser
[19]	SAT	47.8	242	-	Combined with condenser
[14]	SAT	47.5	200.3	1.48	Combined with condenser
[28]	Paraffin	44	174.12	0.13	Combined with condenser
[29]	SAT	58	266	0.43	Combined with condenser
[30]	SAT	58	266	0.43	Combined with condenser
[31]	Paraffin	43	255	0.2	Combined with condenser
[32]	Stearic acid	69	157.5	18.9	Combined with condenser
[33]	Paraffin	40–44	210	0.2	Combined with condenser
[34]	RT42	38–43	165	0.2	Combined with condenser
[35]	Paraffin	52–54	140	5.38	Combined with condenser
[36]	Paraffin	46.7–47.2	144	0.29	Combined with condenser
[37]	CaCl ₂ ·6H ₂ O	29	190.8	1.088	Defrosting
[38]	CaCl ₂ ·6H ₂ O	29	-	-	Defrosting
[39]	Paraffin	48	103	-	Defrosting
[40]	Paraffin	6.17–9.43	134.9–136.1	0.2	Defrosting
[41]	Paraffin	6.17–8.19	134.9–136.1	0.2	Defrosting
[42]	CaCl ₂ ·6H ₂ O	29	176	1.09	Defrosting
[43]	Lauric acid	42	178	0.147	Connected to the condenser
[44]	Paraffin	53	237.5	0.22	Connected to the condenser
[45]	Palmitic acid	57.8–61.8	200	0.28	Connected to the condenser
[46]	CaCl ₂ ·6H ₂ O	32–45	190	-	Connected to the condenser
[47]	Paraffin	51	162	0.85	Provides stable temperature
[48]	CaCl ₂ ·6H ₂ O	29	151.6	3.328	Provides stable temperature
[49]	DSP	37	265	0.514	Connected to the condenser
[50]	CaCl ₂ ·6H ₂ O	29	170	-	Provides stable temperature
[51]	CaCl ₂ ·6H ₂ O	29.7–29.85	187.49	1.008	Provides stable temperature
[52]	CaCl ₂ ·6H ₂ O	29.9	187.49	1.09	Provides stable temperature
[53]	CaCl ₂ ·6H ₂ O	29	187.49	1.088	Provides stable temperature
[54]	SAT	58	250	0.8	Connected to the condenser

3. Performance Improvement Methods of PCMs

If PCMs want to match the heat pump heating system and enhance its thermal physical properties, they must be modified by performance improvement methods. For organic PCMs, high thermal conductivity additives such as carbon nanotubes (CNTs), expanded

graphite (EG) and metal foams are usually added to improve their thermal conductivity. For inorganic PCMs, the most important problem is to solve the problem of supercooling and phase separation. The typical solution is to simultaneously add some nucleating agent and thickener to the PCMs, in order to match the specific temperature range of the heat pump heating system. Adding melting point modifiers to PCMs is an effective method. The encapsulation method can effectively solve the corrosion and leakage problems of inorganic PCMs. Considering the operating characteristics of heat pumps and the thermal terminal temperature requirements, this section reviews the performance improvement methods of PCMs with melting points in the range of 40–60 °C. The PCMs have paraffin wax and SAT, which are commonly used in heat pump-coupled TES systems, ultimately providing a theoretical basis for the practical application of PCMs in heat pump heating systems.

3.1. Additives

In order to solve the problem of the low thermal conductivity of PCMs, many researchers have used additives with high thermal conductivity to improve the thermal performance of PCMs. Basically, there are two types of additives, carbon-based additives and metal-based additives.

3.1.1. PCMs with Carbon-Based Additives

CNTs and carbon nanofibers (CNFs) are two widely researched one-dimensional carbon-based additives with high aspect ratios that build linear heat transfer paths. Döğüşcü et al. [55] used n-hexadecanol (HD) with a melting point of 47 °C as a PCM, with high internal phase emulsion-templated polymer (PHP) as scaffolds and carbon nanofibers as additives. High-performance composite PCMs were prepared showing excellent thermal reliability and chemical stability. As shown in Figure 4a, after adding CNF to PHP foam, its pore structure changed significantly, greatly increasing the interrelation between open pores. Meanwhile, HD was well adsorbed onto the porous skeleton of the composite PCM. Compared with HD, the thermal conductivity of the composite PCM was greatly improved, and the higher the CNF content, the higher the thermal conductivity. Due to the enhanced thermal conductivity, the heat storage and release times of the composite were relatively reduced. Cui et al. [56] made a new type of composite PCM by adding CNT and CNF to paraffin and soy wax, respectively, at a melting point of 52–54 °C. The experimental results showed that CNF could improve the thermal properties of soy wax more effectively than CNT. In addition, compared with pure wax, CNF/PCMs and CNT/PCMs composites had higher thermal conductivity and higher thermal conductivity as mass ratios of CNF and CNT increased, but did not significantly change the latent heat of pure wax. As shown in Figure 4b, although a single CNT is much smaller than a single CNF, it is easier to evenly disperse in the material due to its larger diameter and weaker van der Waals forces. Therefore, CNFs have a better performance in improving the thermal conductivity of the material. Kuziel et al. [57] used three different forms of CNTs as additives in paraffin wax at a melting point of 48–58 °C. Figure 4c shows the microstructure of the composite PCMs. A multi-wall CNT (MWCNT)–paraffin composite PCM with excellent performance was reported with mass ratios of 0.5 wt %, 37% increase in thermal conductivity, 6.3% increase in enthalpy of phase transition and good cycle stability with reduced supercooling. The addition of 2.0 wt % in-house MWCNTs increased the thermal conductivity by up to 161%, but the thermal performance was mediocre in other aspects. At the same time, the increased rate of thermal conductivity did not increase with the increase of the additive mass ratio. In addition, the authors propose that the improved thermal properties of the composites came from the higher crystallinity of individual nanotubes and the larger aspect ratio of the nanotubes. Tang et al. [58] prepared a myristic–stearic acid (MA–SA) binary eutectic with a melting point of 42.7 °C. In order to improve the thermal conductivity of MA–SA eutectic, CNTs were added to the material. Figure 4d shows a photograph of the composite PCMs with CNT added. The authors observed that CNTs clumped easily and formed bundles, so

a magnetic agitator was used to disperse the CNTs, and the eutectic material was adsorbed onto the surface of the CNTs and filled the voids between the CNTs. The addition of CNTs improved the thermal conductivity of the composite PCM and decreased the degree of supercooling, but resulted in a decrease in the latent heat. In the study of PCM theory and modelling, molecular dynamics (MD) is a commonly used method, which is the main method, mainly Newtonian mechanics, to simulate the motion of a molecular system [59]. Klochko et al. [60] used MD to investigate the thermal physical properties of n-hexadecane at different temperature ranges and made a number of experimental measurements, the results of experiments and simulation showed good agreement. Du et al. [61] developed a MD simulation method to predict the structure, diffusion, and thermal properties of composite PCMs based on CNTs, and explained the underlying mechanism of the enhanced thermal properties of CNTs.

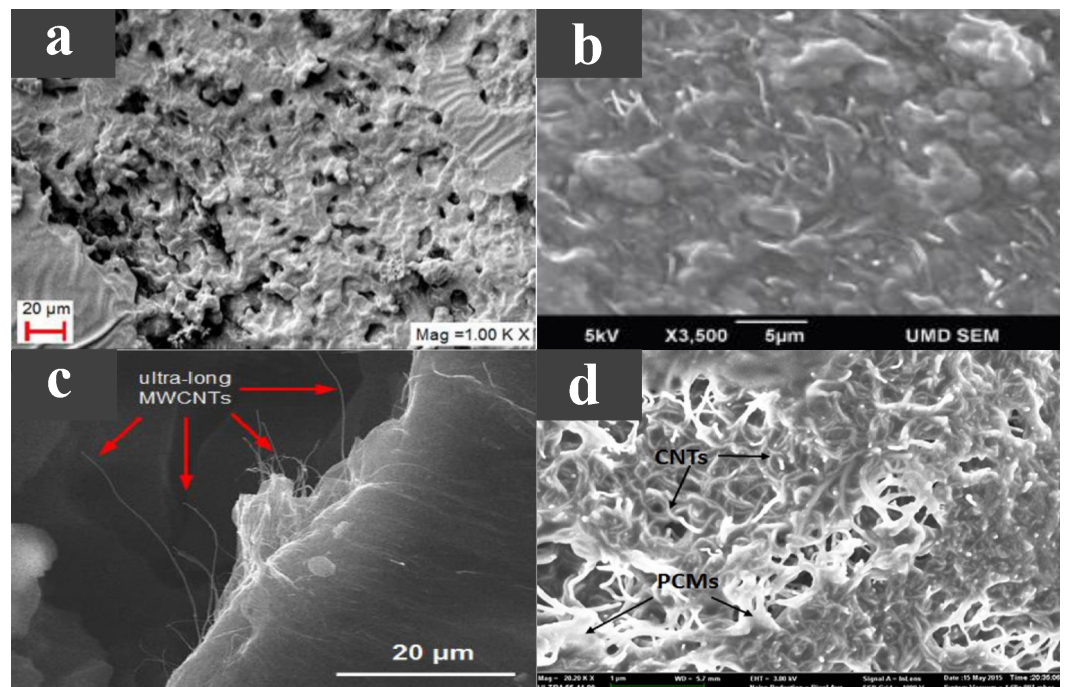


Figure 4. (a) SEM photograph of PHP@CNF/HD [55]. (b) SEM photograph of CNF/soy wax [56]. (c) SEM photograph of paraffin-MWCNTs [57]. (d) SEM photograph of MA-SA/CNTs [58].

The two-dimensional carbon-based additive is also a material with high thermal conductivity, with a transverse size in micrometers and a thickness in nanometres. Considering that the addition of graphene or MWCNT alone may have a limited effect on the thermal properties of PCMs, Zou et al. [62] prepared an MWCNT/graphene-based composite PCM with a phase transition temperature of 40.8–45.3 °C, and determined the optimal ratio of additives. Experiments showed that graphene had greater thermal conductivity than MWCNT, so for the same amount of addition, graphene has a greater increase in the thermal conductivity of the PCM. The PCM's supercooling was slightly reduced by carbon-based additives acting as nucleating agents. Compared with pure paraffin wax and adding an additive alone, the thermal conductivity of the MWCNT/graphene-based composite PCM greatly improved, because the mixed carbon additive could establish an effective three-dimensional heat transfer path and obtain good synergistic enhancement of the heat transfer effect, as shown in Figure 5a. This greatly improves the thermal conductivity of the PCM. Lin et al. [63] used palmitic acid (PA) as a PCM, with nano SiO₂ with an adsorptive capacity as the support material, and added graphene nanoplatelets (GNPs) with enhanced thermal conductivity as an additive to prepare a new type of composite PCM with a melting point of 60 °C. The microscopic morphology of GNP is shown in Figure 5b. It has a lamellar structure, smooth surface, and large specific surface area. The material performance ex-

periments showed that with the increase in GNP content, the shape stability and thermal conductivity of the composite PCM improved, and the composite PCM had excellent thermal stability and chemical reliability, but the latent heat decreased related to the GNP content in the composite PCM. Liu et al. [64] compared the thermal properties of a paraffin/graphene composite PCM and a paraffin/exfoliated graphite sheet composite PCM. The melting points of both composites were around 40 °C. As shown in Figure 5c,d, both graphene and exfoliated graphite sheets exhibit lamellar structures, are evenly distributed in paraffin wax, do not have any micro-cracks or loose interfaces, and are both chemically inert. The experimental results showed that both graphene and exfoliated graphite sheet greatly improved the thermal conductivity of paraffin wax. Because graphene's layered structure is larger than that of the exfoliated graphite sheets, graphene is more conductive than exfoliated graphite sheets. Moreover, with the increase in the additive mass fraction, the enthalpy of the composite PCMs first increased and then decreased, caused by the molecular interactions between the additive and paraffin wax, and the non-melting enthalpy of the additive itself. Zhang et al. [65] investigated the thermophysical properties of paraffin/ethylene–vinyl acetate/graphene nanocomposites using MD simulations. The results showed that the addition of graphene enhanced the thermal conductivity of the PCM; however, in increasing its content, the heat transfer effect may be inhibited.

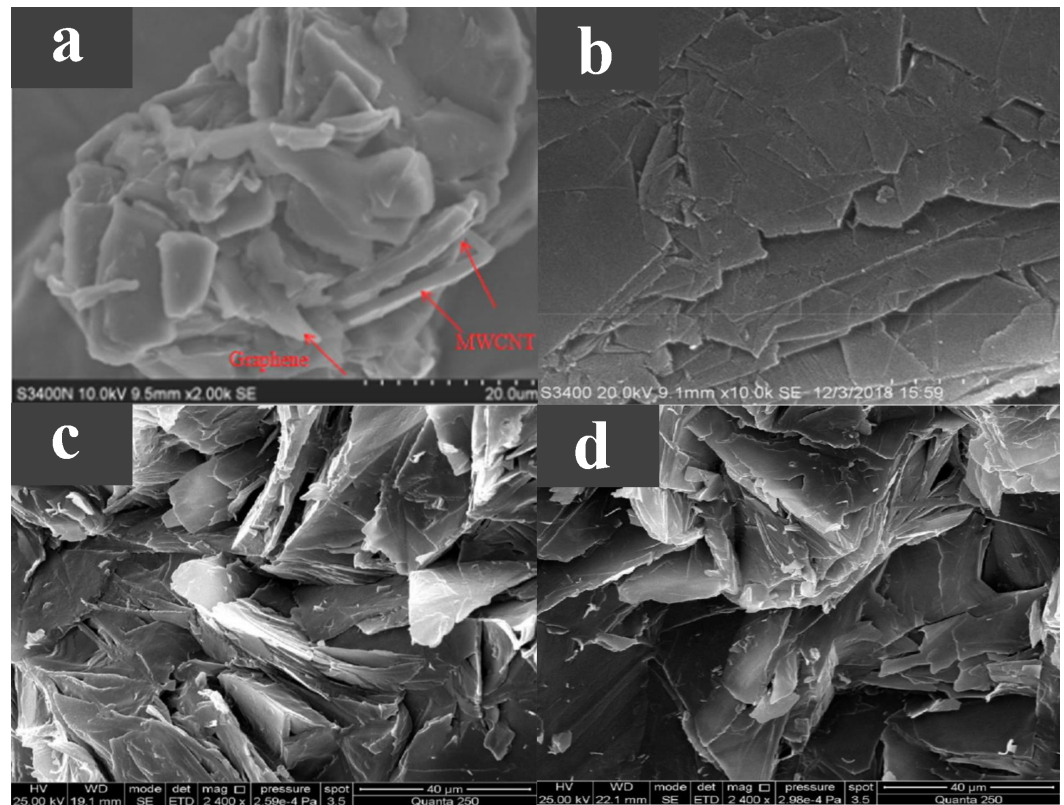


Figure 5. (a) SEM photograph of the PCM with graphene and MWCNT [62]. (b) SEM photograph of GNP [63]. (c) SEM photograph of paraffin/graphene composite, (d) SEM photograph of paraffin/exfoliated graphite sheet composite [64].

Unlike directly dispersing one- or two-dimensional carbon-based additives uniformly into the PCM, three-dimensional carbon-based additives can form a skeleton within the PCM to enhance shape stability, form a network-like heat transfer channel to enhance thermal conductivity, and have higher porosity and specific surface area. Taking paraffin wax with a phase transition temperature of 44.1–47.7 °C as the base material, Huang et al. [66] added 3D a graphene skeleton to improve the shape stability and thermal conductivity of paraffin wax. As shown in Figure 6a,b, due to the interaction between the multilayer-graphene (MG) and the carbon layer, pores were formed on the carbon layer, maintaining

the porous structure, enhancing the mechanical strength and providing better physical adsorption, while the cyclic stability of the composite PCMs was also guaranteed. As the MG content increases from 0.6 to 15.1 wt %, the thermal conductivity continued to increase, reaching the highest of 0.88 W/(m·K). This is because with the increase in MG content, the internal 3D network is more closely combined to form a more continuous heat conduction network, but the latent heat somewhat decreases. Using dodecanoic acid (DA) as a PCM, Atinafu et al. [67] added a graphene framework with high specific surface area and high porosity to produce composite PCMs with a stable shape. The phase transition temperature of the composite PCM was 36.8–45.1 °C. The graphene framework was generated by the pyrolysis and washing of RCOONa. The fabrication process is shown in Figure 6c. Due to the effective heat transfer path in the framework structure, with the increase in the graphene framework content, the thermal conductivity was also higher. Because the graphene framework assists in DA heterogeneous nucleation, the supercooling degree of the composite materials was reduced. The composite PCM also had good thermal reliability and shape stability, but its latent heat was reduced compared with DA.

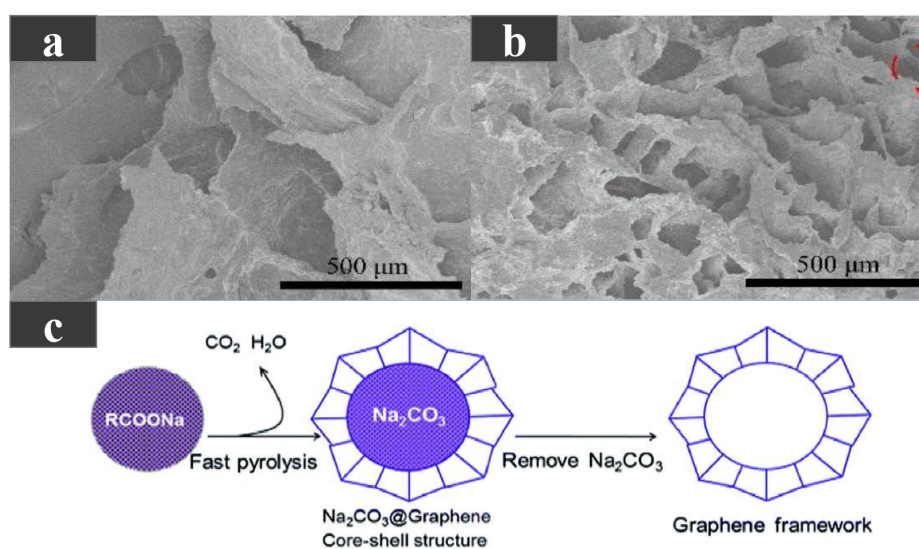


Figure 6. (a) SEM photograph of PCM with 0.6 wt %MG, (b) SEM photograph of PCM with 15.1 wt %MG [66]. (c) Schematic diagram of graphene framework preparation [67].

Yang et al. [68] encapsulated hybrid graphene aerogel (HGA) in three-dimensional graphene foam (GF) to construct three-dimensional mixed GF/HGA (GH) microstructures, and then used GH to fabricate a PW/GH composite PCM with a melting point of around 56 °C. Compared with pure paraffin wax, the thermal conductivity of the composite PCM increased by 574%, and the latent heat slightly reduced. Moreover, after 100 melting and cooling cycle experiments, the composite PCM possessed excellent thermal reliability and chemical stability. Jin et al. [14] used EG to improve the thermal conductivity of SAT–KCl–urea composite salt, and produced a composite PCM with a melting point of 47.5 °C. The composite could be applied in heat pump latent heat thermal energy storage systems. The addition of EG greatly enhanced the thermal conductivity of the SAT–KCl–urea composite salt, which increased from 0.28 to 1.48 W/(m·K). However, as EG did not occur in phase transition, the latent heat of the composite PCM always decreased with the increase in EG content. The SAT–KCl–urea EG composite PCM also had an excellent performance in shape stability and thermal reliability. For air-source heat pump water heaters, to enhance the thermal conductivity of paraffin and to prevent the leakage of paraffin, Wu et al. [35] made an expanded graphite/paraffin composite PCM using paraffin with a melting point of 52–54 °C as the base material and EG as an additive. The thermal conductivity of the composite PCM was 5.38 W/(m·K).

In a word, carbon-based additives are good performance-enhancing materials for PCMs and are mainly used in organic materials. Carbon-based additives can be divided into one-, two- and three-dimensional structural materials, which can greatly improve the thermal conductivity of PCMs, enhance the thermal reliability and shape stability of PCMs, and even reduce the degree of supercooling. However, latent heat reduction is an obvious problem, mainly because carbon-based additives occupy space in the composite PCMs and cannot phase change. Therefore, in practical applications, researchers need to constantly adjust the mass fraction of carbon-based additives and PCMs to determine the optimal ratio.

3.1.2. PCMs with Metal-Based Additives

As a common metal-based additive, metal foam is also a high thermal conductivity material. Huang et al. [69] took myristyl alcohol (MA) as the base PCM and added nickel foam and copper foam to compare the differences in thermal properties between them. As shown in Figure 7a,b, MA is well encapsulated in the metal foam regardless of the additive, and the composite PCMs can be heated/cooled evenly due to the reliable heat transfer path established between MA and the metal foam. The transformation temperature of the composite PCMs was about 40 °C. Compared to pure MA, the thermal conductivity of the MA/nickel foam composite PCM and the MA/copper foam composite PCM increased by 1.80 times and 7.51 times, respectively, at 40 pores per inch. This indicated that the thermal conductivity of copper foam to MA was better than that of nickel foam under the same pore size. At the same time, the smaller the pore size, the higher the thermal conductivity. This is due to that fact that the larger the pore size, the larger the interfacial area, the higher the thermal resistance, and the lower the thermal conductivity. However, the addition of metal foam reduced the latent heat of composite PCMs. This is because the latent heat was provided by MA and the metal foam cannot phase change.

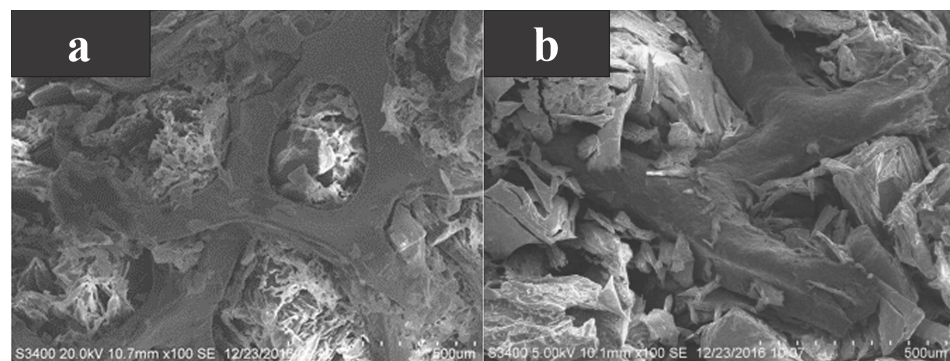


Figure 7. (a) SEM photograph of MA/nickel foam, and (b) SEM photograph of MA/copper foam [69].

Zheng et al. [70] conducted numerical simulation and experimental verification of paraffin/copper foam composite PCMs using two- and three-dimensional computational models, in which the temperature of the phase transition of paraffin wax was 48–50 °C. The experimental and simulation results showed that copper foam can improve the thermal conductivity of paraffin wax, the smaller the porosity, the higher the thermal conductivity of composite PCMs, but copper foam did affect the latent heat of the composite PCMs, that is, the smaller the porosity of copper foam, the less heat energy stored. Paraffin/copper foam composite PCMs and paraffin/nickel foam composite PCMs were made by Ferfera et al. [71] using paraffin wax as the base material at 42–48 °C. Metal foam greatly improves the thermal conductivity of paraffin wax. The thermal conductivity of copper is better than that of nickel, so the thermal conductivity of PCMs enhanced by copper foam is higher than that of nickel foam. Meanwhile, the addition of metal foam can improve the thermal effusivity and thermal diffusivity of composite PCMs. Due to the improvement of the thermal performance of the composite PCMs, the heat rate of the heat exchanger is improved, and the energy is quickly absorbed from the source. However, the decrease in the latent heat of

the composite PCMs lead to a decrease in the heat storage capacity of the heat exchanger. Some researchers have also added metal foams to inorganic PCMs to improve their thermal conductivity. Xiao et al. [72] first prepared a composite PCM (SAT/X) composed of 98% SAT and 2 wt % xanthan gum. In order to improve its thermal conductivity, copper foams were added, as shown in Figure 8. The addition of copper foam resulted in the formation of an efficient thermal conductivity network in the SAT/X/CF composite, and its thermal conductivity was greatly enhanced, with the thermal conductivity of SAT/X/CF reaching $2.10 \text{ W}/(\text{m}\cdot\text{K})$, 176% higher than that of SAT/X. At the same time, after 200 heating and cooling cycles, the composite PCMs still maintained good performance, but the latent heat value decreased. Li et al. [73] first modified SAT and then added copper foam to enhance its thermal conductivity. The experimental results showed that the thermal conductivity of the copper foam/SAT composite PCM was about 11 times higher than that of pure SAT, and the heat transfer time was greatly reduced.

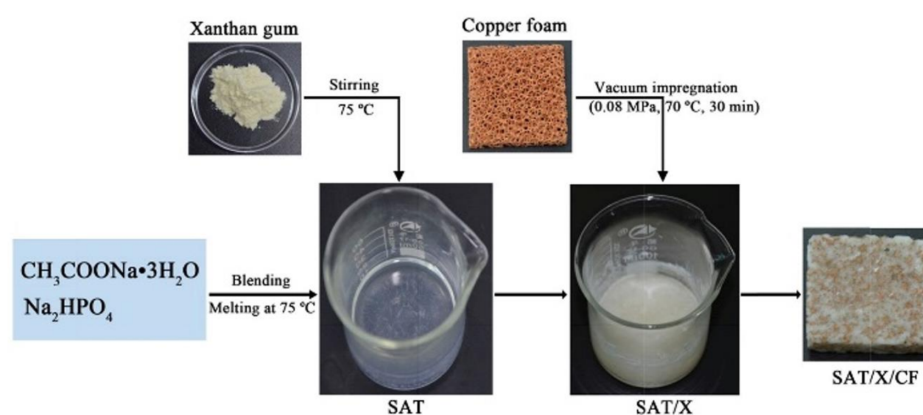


Figure 8. Schematic diagram of SAT/X/CF composite PCM preparation [72].

Many researchers have also used metal nanoparticles and metal oxides as additives to improve the thermal conductivity of PCMs. In order to improve the thermal conductivity of organic materials, Wen et al. [74] added 1, 2, 3 and 4 wt % nano coppers to lauric acid (LA), and the thermal conductivity of the composite PCM increased by 75.0, 106.3, 118.8, and 125%, respectively. With the increase in the weight percentage of copper nanoparticles, the thermal conductivity increases first and then becomes stable, because some copper is oxidized with the increase in copper nanoparticles. The latent heat of the composite PCM is reduced, possibly because the mass of LA is occupied by nano copper, while the copper itself does not undergo a phase transition. After the addition of attapulgite, the thermal stability of the composite PCM is enhanced, and the thermal conductivity of the composite PCM increases up to $0.46 \text{ W}/(\text{m}\cdot\text{K})$, synergistically enhanced by attapulgite and nano copper. Tang et al. [75] prepared a composite PCM with stearic acid (SA) as the PCM and titanium dioxide (TiO_2) as an additive for heat storage in buildings. The melting point of SA/ TiO_2 composite PCM was $53.84 \text{ }^\circ\text{C}$. Due to the additives, the latent heat of the composite PCM was greatly reduced, but its supercooling degree was also reduced. In addition, TiO_2 , as a supporting material, established a protective barrier on the surface of the composite PCM, enhancing its non-flammability and thermal reliability, making it suitable for being applied to building heat storage. Zhao et al. [76] manufactured an Al_2O_3 /PW composite PCM. The porous structure of Al_2O_3 enhanced the anti-leakage performance of the composite PCM and greatly improved the thermal conductivity. When the mass ratio of Al_2O_3 additive reached 50 wt %, the thermal conductivity of the composite PCM increased to $1.27 \text{ W}/(\text{m}\cdot\text{K})$, and its cycle stability also had good performance. However, with the increase in the additive mass ratio, the latent heat of the composite PCM decreased. Li et al. [77] used equilibrium and non-equilibrium MD simulations to investigate the thermal properties of a nano-fluid mixture of n-octadecane and copper nanoparticles. The results showed that copper nanoparticles could improve the thermal properties of

n-octadecane. Liu et al. [78] used MD simulations to study the phase transitions in copper oxide nanoparticles using a porous carbon matrix containing paraffin as a PCM. The results showed that the addition of copper oxide nanoparticles improved the thermal physical characteristics of the PCM.

In conclusion, metal-based additives can improve the thermal conductivity of PCMs, especially for organic materials, and greatly enhance the shape stability of PCMs. Metal-based additives also reduce the latent heat of PCMs; however, oxidation and corrosion may occur. In heat pump heating applications, the pore size of the metal foam must be considered, because it will affect the energy storage capacity and thermal conductivity of composite PCMs.

3.1.3. PCMs with Other Additives

In the practical application of heat pump heating, the ideal melting point of PCMs should be determined first according to the heating performance of the heat pump and the water temperature requirement of the thermal end of the building. However, the actual melting point of PCMs does not match the ideal melting point. Many researchers add various additives to PCMs to change the melting point, to achieve the purpose of temperature range matching, so as to meet the needs of different applications. At the same time, the high degree of supercooling and phase separation will seriously affect the performance of inorganic materials. Therefore, thickener and nucleating agent are an effective way to solve this problem.

The phase transition temperature of SAT was decreased by adding urea. Fu et al. [79] added urea at different mass fractions to SAT to create the SAT–urea mixture, disodium phosphate dodecahydrate (DSP) and sucrose were used as thickening and nucleating agents, respectively. The results of the DSC experiments showed that the phase transition temperature of the mixture changed by changing the mass fraction of urea, adjusted from 49 to 58 °C. The melting point of the mixture decreased with the increase in urea content, and the latent heat also decreased, thus showing so it is necessary to determine the optimal mass fraction of the additive according to the actual situation. Jin et al. [14] added 8 wt % potassium chloride and 3 wt % urea to SAT to synthesize a SAT–KCl–urea mixture, which reduced the melting point of SAT to 47.6 °C. Meanwhile, DSP and carboxyl methyl cellulose (CMC) were used as nucleating and thickening agents, respectively. The mass fraction of CMC needs to be strictly determined, because too little will cause insufficient viscosity of the mixture and phase separation, and too much will reduce the latent heat. Hence, 2 wt % CMC was finally determined. Li et al. [73] added 2.0 wt % disodium hydrogen phosphate dodecahydrate (DHPD) and 0.5 wt % CMC to SAT, as nucleating and thickening agents, respectively, to solve the supercooling and phase separation problem. The supercooling degree of the modified SAT reduced from 3.78 to 2.54 °C, the melting point was maintained between 57 and 58 °C after cyclic tests, and the latent heat first slowly decreased and then plateaued at 258 kJ/kg. Jin et al. [27] added DHPD and CMC to SAT as nucleating and thickening agents, and adjusted the melting point of SAT by using formamide (FA) and acetamide (AC), respectively, to produce a series of composite PCMs with different mass ratios. The experimental results showed that the addition of FA or AC changed the phase transition temperature of SAT, and the optimum mass fraction of the nucleating and thickening agents was discussed. The authors recommended the use of 6 wt % DHPD and 4 wt % DHPD and 4 wt % CMC for the SAT-FA and SAT-AC mixtures, respectively.

3.2. Encapsulation

3.2.1. Work Principle of EPCMs

PCMs are promising materials, but they may be subject to some health limitations when applied in the field of human settlements and buildings. Some kinds of paraffin contain volatile compounds and long-term exposure to their volatiles can be dangerous, although various salt hydrates are generally non-toxic but can cause skin or eye irritation and respiratory problems [80]. At the same time, the problems of supercooling and phase

separation of inorganic PCMs also limit the application of this technology. The encapsulation of PCMs can solve these problems. Encapsulated PCMs (EPCMs) are composed of a core (PCM) and a shell. The shell materials are usually classified as organic, inorganic, or hybrid organic–inorganic shells. The following takes solid–liquid materials as an example. The core material of EPCMs changes from a solid to a liquid after absorbing heat during heating, while the shell material remains solid without deformation; therefore, EPCMs still appear as solid particles. Under exothermic conditions, the core material is converted from a liquid to a solid, thus releasing heat, completing the heat storage–release process [81]. The purpose of encapsulation is to maintain the stable shape of the PCM and isolate it from the surrounding environment to prevent changes in the PCMs; meanwhile, encapsulation can increase the heat transfer area of PCMs, improve the heat transfer rate, and enhance the thermal and mechanical stability of PCMs, as well as reduce corrosion, seal some PCMs that cannot be used directly or have dangerous properties, and expand the application range of PCMs [82].

According to the diameter of the microcapsule, it can be divided into three types: macro-encapsulated PCMs (greater than 1 mm), micro-encapsulated PCMs (1–1000 μm), and nano-encapsulated PCMs (1–1000 nm) [83].

The main encapsulation methods are physico-mechanical, chemical, and physico-chemical. Physical-mechanical methods include spray drying, centrifugal extrusion, vibrational nozzle, and solvent evaporation; chemical methods include in situ polymerization, emulsion polymerization, suspension polymerization, interfacial polymerization, and electroplating; while physical-chemical methods include sol-gel, coacervation, and ionic gelation processes [12,84].

3.2.2. Encapsulation of PCMs

Encapsulation can effectively improve the phase separation and supercooling problems of inorganic salt hydrates, and enhance the thermal stability and mechanical strength of PCMs. In order to solve the problems of phase separation and the high subcooling degree of sodium thiopulate pentahydrate (STP), Liu et al. [85] encapsulated STP as the core and silica shell by the sol-gel method, successfully manufacturing microcapsule PCMs (MEPCMs) with a phase change temperature of 46.41–47.69°. An SEM image of the microcapsule is shown in Figure 9a,b. It can be seen that the microcapsule presents a regular spherical shape, and its edge is the crystal structure of the silica shell. After micro-encapsulation, the heat transfer area of STP increases and the thermal conductivity of silica is higher than STP, so the thermal conductivity of the microcapsules is improved, the degree of supercooling is reduced, and the thermal stability is enhanced.

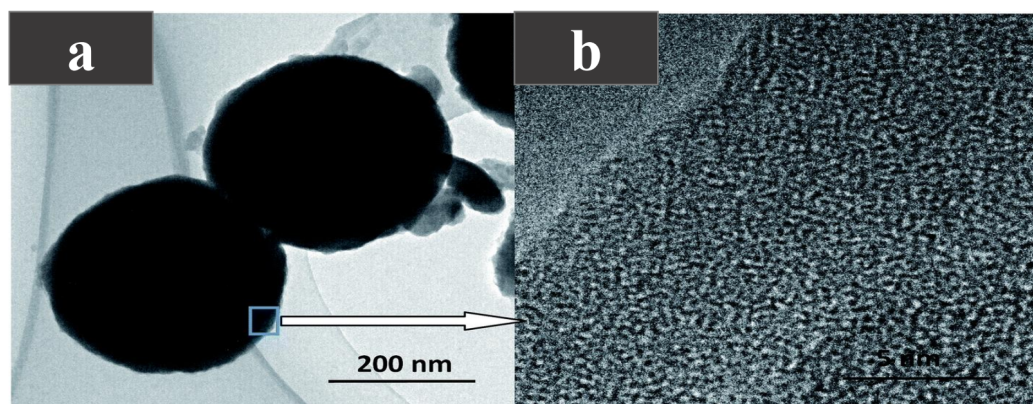


Figure 9. (a) TEM photograph of the micro-PCM, (b) TEM photograph of the crystal structure [85].

$\text{Na}_2\text{HPO}_4 \cdot 7\text{H}_2\text{O}$ is a PCM with a high-energy storage density and a suitable melting point ($52.3\text{ }^\circ\text{C}$). Fang et al. [86] used $\text{Na}_2\text{HPO}_4 \cdot 7\text{H}_2\text{O}$ as the core PCM and SiO_2 as the shell, successfully manufacturing a new type of MEPCM by using a one-pot method. MEPCM has a melting point of $50.12\text{ }^\circ\text{C}$ and a melting enthalpy of 159.8 kJ/kg . With the increase in the mass ratio of the core material to the shell material, the thermal conductivity of the MEPCM continued to rise and reaching up to $0.3838\text{ W/(m}\cdot\text{K)}$. Liu et al. [87] micro-encapsulated DSP with silica through interfacial polymerization combined with the sol-gel process. the encapsulation rate (ER) and encapsulation efficiency (EE) were used to evaluate the performance of the encapsulated PCM and were very important parameters. The experimental results showed that when the core-shell ratio was 4:1, the EE of the microcapsule was 75.3%, the melting point of the material was $57.4\text{ }^\circ\text{C}$, the melting enthalpy was 177.0 kJ/kg , and the thermal conductivity was $0.5004\text{ W/(m}\cdot\text{K)}$. A more compact shell and a larger core loading rate resulted in higher thermal conductivity of the microcapsules, as a higher loading rate represents a higher filling degree of the PCM in the microcapsule core. The heating-cooling cycle test proved that the thermal stability of microcapsules was improved. Fu et al. [88] successfully synthesized a new type of MEPCM with STP as the core and poly(ethyl-2-cyanoacrylate) (PECA) as the shell, with a melting point range of $44.8\text{--}46.71\text{ }^\circ\text{C}$. Compared with STP, the latent heat of the microcapsules was significantly reduced because the PECA shell did not undergo a phase transition, and only the STP in the core contributed latent heat through a phase transition. Therefore, the latent heat of microcapsules was mainly determined by the core load, and it was also found that the latent heat of microcapsules first increases and then decreases with the increase in core content. The heating-cooling cycle experiment showed that the microcapsules have a slight improvement in thermal stability and reliability. Organic PCMs can also be encapsulated to improve the thermal stability and reliability of PCMs. Lauric acid (LA) is an environmentally friendly PCM. Sami et al. [89] prepared MEPCMs with LA as the core and polystyrene as the shell through an optimized emulsion polymerization process. The operating variables, such as the mass ratio of materials and stirring speed, were optimized to obtain an MEPCM with a melting point of $43.77\text{ }^\circ\text{C}$ and a latent heat of 167.26 kJ/kg . The microcapsule shell provided excellent protection for the core while enhancing the thermal stability of the MEPCM. In addition, Zhang et al. [90] synthesized a series of nano-PCMs with paraffin as the core and melamine and formaldehyde as the shell by the in situ polymerization method. Nano-PCMs have a melting point of about $49\text{ }^\circ\text{C}$. The results showed that the nano-PCMs had an excellent latent heat and encapsulation rate, up to 135.3 kJ/kg and 74.1%, respectively. After 2000 thermal cycle tests, the melting and freezing temperatures and latent heat of the nano-PCMs only slightly changed, indicating that the material had good thermal reliability. As shown in Figure 10, the microstructure of the nano-PCMs was not damaged after the cyclic experiments, indicating that the material as a whole had good mechanical properties. EPCMs with eutectic PCMs as the core were also prepared by some researchers. Chen et al. [91] prepared STP-SAT eutectic hydrated salts with mass fractions of 72 and 28%, respectively. The eutectic had a high enthalpy (211.9 kJ/kg) and a suitable phase transition temperature ($41.58\text{ }^\circ\text{C}$), and 2% $\text{SrCl}_2 \cdot 6\text{H}_2\text{O}$ was added as a nucleating agent to promote the crystallization of the PCMs. Solid polyurethane was used to encapsulate the eutectic and solve leakage and corrosion problems. Rao et al. [92,93] used MD simulation to study the thermal properties of nanocapsules with SiO_2 as the shell and n-octadecane, n-nonadecane, n-eicosane, n-heneicosane or n-docosane as the core. The results showed that the proposed MD simulation can help optimize the performance of PCMs.

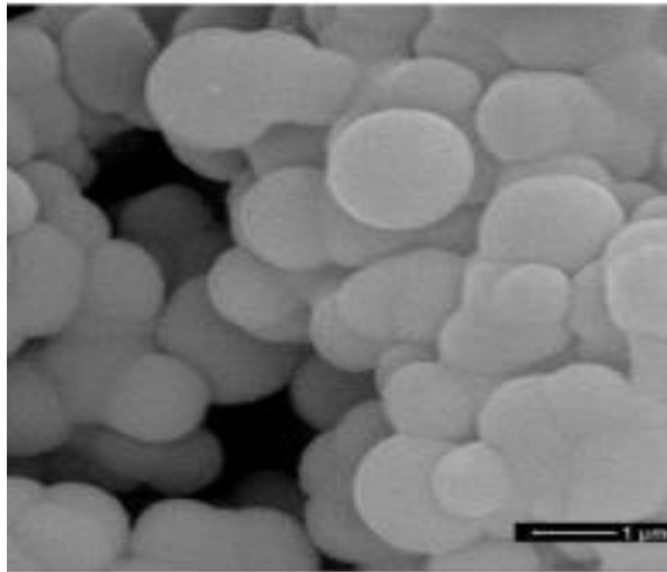


Figure 10. SEM photograph of nano-PCMs after 2000 thermal cycles [90].

3.3. Eutectic PCMs

When considering the most desirable PCMs for a heat pump heating system, there may be situations where the PCMs do not have the favourable properties required for use in real applications. Each PCM has a certain melting point and latent heat, and they can only be used in specific applications, thus limiting the application of PCMs. Whereas by mixing two or more PCMs to create eutectic PCMs, the melting temperature and latent heat can be tailored [94], thus making them suitable for specific applications. The main problem with eutectic mixtures is the lack of experimental data on their thermophysical properties, which can be predicted from the thermophysical properties of the individual components using simplified correlations [95].

4. Conclusions and Perspectives

Single PCMs have fixed thermophysical properties that may not match the requirements of real applications, so various performance improvement methods are needed to modify PCMs. This paper reviews the performance improvement methods of PCMs applied to heat pump heating systems, the main conclusions are as follows:

- When selecting PCMs for heat pump heating systems, the melting point is the first thing that should be considered, which is related to the performance of the heat pump and the temperature requirements of the thermal end of the building. Thermal conductivity and latent heat need to be focused on, which will affect the heat transfer efficiency between the PCMs and HTF and the heat storage capacity of the TES system, respectively. Meanwhile, some defects of PCMs need to be paid attention to, such as the supercooling, phase separation, and corrosion of inorganic PCMs, which are related to the working efficiency and life cycle of the TES system.
- Carbon- and metal-based additives are efficient thermal conductivity-enhancing materials. Carbon-based additives are classified as one-, two-, and three-dimensional materials. Overall, the three-dimensional carbon-based materials have the greatest enhancement effect on thermal conductivity, which can form a network heat transfer channel. Metal-based materials have high thermal conductivity and can be used as additives to improve the thermal conductivity of PCMs. However, the increase in additive content will inevitably reduce the latent heat of the composite PCMs, so it is necessary to adjust the additive mass fraction according to the actual situation, and finally obtain the ideal composite PCM. Nucleating and thickening agents are important materials to solve the problems of supercooling and phase separation of

inorganic PCMs; consequently, the mass fraction of additives needs to be constantly adjusted. Melting point regulators are also used appropriately in SAT to give PCMs with a desired melting point.

- Encapsulation is a promising technology which can effectively solve the problem of supercooling and phase separation of inorganic PCMs, and avoid damage to PCMs. The mass ratio of the core–shell material must be considered, which will affect the thermal conductivity and latent heat of the EPCMs. In addition, when PCMs are used in heat pump heating systems, encapsulation makes it possible to use corrosive or toxic materials.
- By mixing two or more PCMs to make eutectic PCMs, the melting point and latent heat of the material can be arbitrarily adjusted to suit different heat pump heating scenarios. The thermophysical properties of eutectic PCMs can be predicted by simple correlation formulae.

In the future, the coupling of heat pump and phase change energy storage technologies has broad application prospects. The use of PCMs can realize heat storage and release, to meet the diversified needs of terminal energy consumption, and the performance improvement methods of PCMs ensures the efficient application of this technology. The prospects for this technology are as follows:

- Through theoretical research and experimental methods, matching the operation characteristics of heat pumps and PCM energy storage characteristics, the optimal design parameters of PCM thermal physical characteristics can be obtained, and PCMs can be transformed by performance improvement methods.
- When selecting a PCM suitable for a heat pump heating system, the multi-criteria decision-making method is a scientific and efficient screening method, which can obtain the most appropriate PCM according to the needs of decision-makers, but early data statistics need to be given priority consideration.
- The efficient control strategy of a heat pump-coupled energy storage system is of great significance for the development of this technology. The use of advanced algorithms to constantly search for the optimal working point of the system, while meeting the energy consumption needs of users, reduce costs, and realize flexible interactions with the power grid, has huge development potential.

Author Contributions: C.Z.: Conceptualization, methodology, writing—original draft. Y.L.: methodology, writing—original draft, writing—review and editing, visualization. F.W.: conceptualization, project administration, funding acquisition, supervision. Z.W.: investigation, writing—review and editing. Q.X.: investigation, visualization. Y.Z.: project administration, resources. J.L.: formal analysis, resources. B.L.: data curation. W.C.: conceptualization, writing—review and editing. All authors have read and agreed to the published version of the manuscript.

Funding: This research is financially supported by the QinChuanyuan ‘Scientist + Engineer’ team project (2022KXJ-039) and Innovation Capability Support Program of Shaanxi Province (2021PT-028), Social Development Demonstration Project on Science and Technology Innovation of Xi’an (20SFSF0017), and the Open Project of Key Laboratory of Coal Resources Exploration and Comprehensive Utilization (KF2021-1).

Institutional Review Board Statement: Not applicable.

Informed Consent Statement: Not applicable.

Data Availability Statement: The data can be available if there is any request.

Conflicts of Interest: The authors declare no conflict of interest.

Abbreviations

The following abbreviations are used in this manuscript:

TES	Thermal energy storage
PCMs	Phase change materials
GHG	Greenhouse gases
ET	Energy transition
HP	Heat pump
ASHP	Air source heat pump
GSHP	Ground source heat pump
DR	Demand response
DSM	Demand-side management
COP	Coefficient of performance
SAT	Sodium acetate trihydrate
HTF	Heat transfer fluid
MD	Molecular dynamics
CNTs	Carbon nanotubes
EG	Expanded graphite
CNFs	Carbon nanofibers
HD	n-Hexadecanol
PHP	High internal phase emulsion-templated polymer
MWCNT	Multi-wall carbon nanotube
MA-SA	Myristic–stearic acid
GNPs	Graphene nanoplatelets
MG	Multilayer-graphene
DA	Dodecanoic acid
HGA	Hybrid graphene aerogel
GF	Graphene foam
MA	Myristyl alcohol
DSP	Disodium phosphate dodecahydrate
CMC	Carboxyl methyl cellulose
DHPD	Disodium hydrogen phosphate dodecahydrate
FA	Formamide
AC	Acetamide
EPCMs	Encapsulated phase change materials
STP	Sodium thiosulfate pentahydrate
MEPCM	Microcapsule phase change material
PECA	Poly(ethyl-2-cyanoacrylate)
LA	Lauric acid

References

- Salvia, M.; Reckien, D.; Pietrapertosa, F.; Eckersley, P.; Spyridaki, N.A.; Krook-Riekkola, A.; Olazabal, M.; Hurtado, S.D.G.; Simoes, S.G.; Geneletti, D.; et al. Will climate mitigation ambitions lead to carbon neutrality? An analysis of the local-level plans of 327 cities in the EU. *Renew. Sustain. Energy Rev.* **2021**, *135*, 110253. [[CrossRef](#)]
- De La Peña, L.; Guo, R.; Cao, X.; Ni, X.; Zhang, W. Accelerating the energy transition to achieve carbon neutrality. *Resour. Conserv. Recycl.* **2022**, *177*, 105957. [[CrossRef](#)]
- Huo, T.; Cai, W.; Zhang, W.; Wang, J.; Zhao, Y.; Zhu, X. How does income level impact residential-building heating energy consumption? Micro-level evidence from household surveys. *Environ. Impact Assess. Rev.* **2021**, *91*, 106659. [[CrossRef](#)]
- Sadeghi, H.; Ijaz, A.; Singh, R.M. Current status of heat pumps in Norway and analysis of their performance and payback time. *Sustain. Energy Technol. Assessments* **2022**, *54*, 102829. [[CrossRef](#)]
- Wang, Z.; Wang, F.; Liu, J.; Li, Y.; Wang, M.; Luo, Y.; Ma, L.; Zhu, C.; Cai, W. Energy analysis and performance assessment of a hybrid deep borehole heat exchanger heating system with direct heating and coupled heat pump approaches. *Energy Convers. Manag.* **2023**, *276*, 116484. [[CrossRef](#)]
- Ma, L.; Wang, F.; Wang, Z.; Zhang, S.; Liu, Z.; Lou, Y. Experimental investigation on an air source heat pump system with coupled liquid-storage gas-liquid separator regarding heating and defrosting performance. *Int. J. Refrig.* **2022**, *134*, 176–188. [[CrossRef](#)]
- Xu, L.; Pu, L.; Zarrella, A.; Zhang, D.; Zhang, S. Experimental study on the thermal imbalance and soil temperature recovery performance of horizontal stainless-steel ground heat exchanger. *Appl. Therm. Eng.* **2022**, *200*, 117697. [[CrossRef](#)]

8. Vivian, J.; Prativiera, E.; Cunsolo, F.; Pau, M. Demand Side Management of a pool of air source heat pumps for space heating and domestic hot water production in a residential district. *Energy Convers. Manag.* **2020**, *225*, 113457. [[CrossRef](#)]
9. Liu, X.; Zhu, J.; Wang, J.; Fu, Y.; Zhang, H.; Niu, J. Zero fluctuation: Electric-fluctuation-elimination heat pump system with water storage tank based on time-of-use tax. *Energy Build.* **2023**, *279*, 112703. [[CrossRef](#)]
10. Qu, M.; Lu, M.; Li, Z.; Song, X.; Chen, J.; Ziviani, D.; Braun, J.E. Thermal energy storage based (TES-based) reverse cycle defrosting control strategy optimization for a cascade air source heat pump. *Energy Build.* **2020**, *219*, 110014. [[CrossRef](#)]
11. Arteconi, A.; Hewitt, N.J.; Polonara, F. Domestic demand-side management (DSM): Role of heat pumps and thermal energy storage (TES) systems. *Appl. Therm. Eng.* **2013**, *51*, 155–165. [[CrossRef](#)]
12. Nazir, H.; Batool, M.; Osorio, F.J.B.; Isaza-Ruiz, M.; Xu, X.; Vignarooban, K.; Phelan, P.; Kannan, A.M. Recent developments in phase change materials for energy storage applications: A review. *Int. J. Heat Mass Transf.* **2019**, *129*, 491–523. [[CrossRef](#)]
13. Zhou, D.; Zhao, C.Y.; Tian, Y. Review on thermal energy storage with phase change materials (PCMs) in building applications. *Appl. Energy* **2012**, *92*, 593–605. [[CrossRef](#)]
14. Jin, X.; Xiao, Q.; Xu, T.; Huang, G.; Wu, H.; Wang, D.; Liu, Y.; Zhang, H.; Lai, A.C. Thermal conductivity enhancement of a sodium acetate trihydrate–potassium chloride–urea/expanded graphite composite phase–change material for latent heat thermal energy storage. *Energy Build.* **2021**, *231*, 110615. [[CrossRef](#)]
15. Ermel, C.; Bianchi, M.V.; Cardoso, A.P.; Schneider, P.S. Thermal storage integrated into air-source heat pumps to leverage building electrification: A systematic literature review. *Appl. Therm. Eng.* **2022**, *215*, 118975. [[CrossRef](#)]
16. Osterman, E.; Stritih, U. Review on compression heat pump systems with thermal energy storage for heating and cooling of buildings. *J. Energy Storage* **2021**, *39*, 102569. [[CrossRef](#)]
17. Xu, C.; Zhang, H.; Fang, G. Review on thermal conductivity improvement of phase change materials with enhanced additives for thermal energy storage. *J. Energy Storage* **2022**, *51*, 104568. [[CrossRef](#)]
18. Han, L.; Zhang, X.; Ji, J.; Ma, K. Research progress on the influence of nano-additives on phase change materials. *J. Energy Storage* **2022**, *55*, 105807. [[CrossRef](#)]
19. Li, M.; Lin, Z.; Sun, Y.; Wu, F.; Xu, T.; Wu, H.; Zhou, X.; Wang, D.; Liu, Y. Preparation and characterizations of a novel temperature-tuned phase change material based on sodium acetate trihydrate for improved performance of heat pump systems. *Renew. Energy* **2020**, *157*, 670–677. [[CrossRef](#)]
20. Pardiñas, Á.Á.; Alonso, M.J.; Diz, R.; Kvalsvik, K.H.; Fernández-Seara, J. State-of-the-art for the use of phase-change materials in tanks coupled with heat pumps. *Energy Build.* **2017**, *140*, 28–41. [[CrossRef](#)]
21. Moreno, P.; Solé, C.; Castell, A.; Cabeza, L.F. The use of phase change materials in domestic heat pump and air-conditioning systems for short term storage: A review. *Renew. Sustain. Energy Rev.* **2014**, *39*, 1–13. [[CrossRef](#)]
22. Shen, J.; Qian, Z.; Xing, Z.; Yu, Y.; Ge, M. A review of the defrosting methods of air source heat pumps using heat exchanger with phase change material. *Energy Procedia* **2019**, *160*, 491–498. [[CrossRef](#)]
23. Mesalhy, O.; Lafdi, K.; Elgafy, A.; Bowman, K. Numerical study for enhancing the thermal conductivity of phase change material (PCM) storage using high thermal conductivity porous matrix. *Energy Convers. Manag.* **2005**, *46*, 847–867. [[CrossRef](#)]
24. Long, J.Y.; Zhu, D.S. Numerical and experimental study on heat pump water heater with PCM for thermal storage. *Energy Build.* **2008**, *40*, 666–672. [[CrossRef](#)]
25. Agyenim, F.; Hewitt, N. The development of a finned phase change material (PCM) storage system to take advantage of off-peak electricity tariff for improvement in cost of heat pump operation. *Energy Build.* **2010**, *42*, 1552–1560. [[CrossRef](#)]
26. Kelly, N.J.; Tuohy, P.G.; Hawkes, A.D. Performance assessment of tariff-based air source heat pump load shifting in a UK detached dwelling featuring phase change-enhanced buffering. *Appl. Therm. Eng.* **2014**, *71*, 809–820. [[CrossRef](#)]
27. Jin, X.; Wu, F.; Xu, T.; Huang, G.; Wu, H.; Zhou, X.; Wang, D.; Liu, Y.; Lai, A.C. Experimental investigation of the novel melting point modified Phase–Change material for heat pump latent heat thermal energy storage application. *Energy* **2021**, *216*, 119191. [[CrossRef](#)]
28. Li, Y.; Zhang, N.; Ding, Z. Investigation on the energy performance of using air-source heat pump to charge PCM storage tank. *J. Energy Storage* **2020**, *28*, 101270. [[CrossRef](#)]
29. Li, Y.; Huang, G.; Wu, H.; Xu, T. Feasibility study of a PCM storage tank integrated heating system for outdoor swimming pools during the winter season. *Appl. Therm. Eng.* **2018**, *134*, 490–500. [[CrossRef](#)]
30. Li, Y.; Ding, Z.; Du, Y. Techno-economic optimization of open-air swimming pool heating system with PCM storage tank for winter applications. *Renew. Energy* **2020**, *150*, 878–890. [[CrossRef](#)]
31. Zou, D.; Ma, X.; Liu, X.; Zheng, P.; Cai, B.; Huang, J.; Guo, J.; Liu, M. Experimental research of an air-source heat pump water heater using water-PCM for heat storage. *Appl. Energy* **2017**, *206*, 784–792. [[CrossRef](#)]
32. Inkeri, E.; Tynjälä, T.; Nikku, M. Numerical modeling of latent heat thermal energy storage integrated with heat pump for domestic hot water production. *Appl. Therm. Eng.* **2022**, *214*, 118819. [[CrossRef](#)]
33. Yu, M.; Zhang, C.; Fan, Y.; Zhang, X.; Zhao, Y. Performance study of phase change charging/discharging processes of condensing heat storage in cold regions based on a mathematical model. *Appl. Therm. Eng.* **2021**, *182*, 115805. [[CrossRef](#)]
34. Koşan, M.; Aktaş, M. Experimental investigation of a novel thermal energy storage unit in the heat pump system. *J. Clean. Prod.* **2021**, *311*, 127607. [[CrossRef](#)]
35. Wu, J.; Feng, Y.; Liu, C.; Li, H. Heat transfer characteristics of an expanded graphite/paraffin PCM-heat exchanger used in an instantaneous heat pump water heater. *Appl. Therm. Eng.* **2018**, *142*, 644–655. [[CrossRef](#)]

36. Lin, Y.; Fan, Y.; Yu, M.; Jiang, L.; Zhang, X. Performance investigation on an air source heat pump system with latent heat thermal energy storage. *Energy* **2022**, *239*, 121898. [[CrossRef](#)]
37. Minglu, Q.; Liang, X.; Deng, S.; Yiqiang, J. Improved indoor thermal comfort during defrost with a novel reverse-cycle defrosting method for air source heat pumps. *Build. Environ.* **2010**, *45*, 2354–2361. [[CrossRef](#)]
38. Wenju, H.; Yiqiang, J.; Minglu, Q.; Long, N.; Yang, Y.; Shiming, D. An experimental study on the operating performance of a novel reverse-cycle hot gas defrosting method for air source heat pumps. *Appl. Therm. Eng.* **2011**, *31*, 363–369. [[CrossRef](#)]
39. Liu, Z.; Fan, P.; Wang, Q.; Chi, Y.; Zhao, Z.; Chi, Y. Air source heat pump with water heater based on a bypass-cycle defrosting system using compressor casing thermal storage. *Appl. Therm. Eng.* **2018**, *128*, 1420–1429. [[CrossRef](#)]
40. Qu, M.; Tang, Y.; Zhang, T.; Li, Z.; Chen, J. Experimental investigation on the multi-mode heat discharge process of a PCM heat exchanger during TES based reverse cycle defrosting using in cascade air source heat pumps. *Appl. Therm. Eng.* **2019**, *151*, 154–162. [[CrossRef](#)]
41. Minglu, Q.; Rao, Z.; Jianbo, C.; Yuanda, C.; Xudong, Z.; Tongyao, Z.; Zhao, L. Experimental analysis of heat coupling during TES based reverse cycle defrosting method for cascade air source heat pumps. *Renew. Energy* **2020**, *147*, 35–42. [[CrossRef](#)]
42. Hu, W.; Song, M.; Jiang, Y.; Yao, Y.; Gao, Y. A modeling study on the heat storage and release characteristics of a phase change material based double-spiral coiled heat exchanger in an air source heat pump for defrosting. *Appl. Energy* **2019**, *236*, 877–892. [[CrossRef](#)]
43. Teamah, H.; Lightstone, M. Numerical study of the electrical load shift capability of a ground source heat pump system with phase change thermal storage. *Energy Build.* **2019**, *199*, 235–246. [[CrossRef](#)]
44. Dogkas, G.; Konstantaras, J.; Koukou, M.K.; Vrachopoulos, M.G.; Pagkalos, C.; Stathopoulos, V.N.; Pandis, P.K.; Lymperis, K.; Coelho, L.; Rebola, A. Development and experimental testing of a compact thermal energy storage tank using paraffin targeting domestic hot water production needs. *Therm. Sci. Eng. Prog.* **2020**, *19*, 100573. [[CrossRef](#)]
45. Hirmiz, R.; Teamah, H.; Lightstone, M.; Cotton, J. Analytical and numerical sizing of phase change material thickness for rectangular encapsulations in hybrid thermal storage tanks for residential heat pump systems. *Appl. Therm. Eng.* **2020**, *170*, 114978. [[CrossRef](#)]
46. Benli, H.; Durmuş, A. Evaluation of ground-source heat pump combined latent heat storage system performance in greenhouse heating. *Energy Build.* **2009**, *41*, 220–228. [[CrossRef](#)]
47. Sivakumar, M.; Mahalingam, S.; Mohanraj, M. Energy, financial and environmental impact analysis of solar thermal heat pump systems using a direct expansion packed bed evaporator-collector. *Sol. Energy* **2022**, *232*, 154–168. [[CrossRef](#)]
48. Wu, J.; Xian, T.; Liu, X. All-weather characteristic studies of a direct expansion solar integrated air source heat pump system based on PCMs. *Sol. Energy* **2019**, *191*, 34–45. [[CrossRef](#)]
49. Yao, J.; Xu, H.; Dai, Y.; Huang, M. Performance analysis of solar assisted heat pump coupled with build-in PCM heat storage based on PV/T panel. *Sol. Energy* **2020**, *197*, 279–291. [[CrossRef](#)]
50. Kaygusuz, K. Experimental and theoretical investigation of a solar heating system with heat pump. *Renew. Energy* **2000**, *21*, 79–102. [[CrossRef](#)]
51. Esen, M. Thermal performance of a solar-aided latent heat store used for space heating by heat pump. *Sol. Energy* **2000**, *69*, 15–25. [[CrossRef](#)]
52. Han, Z.; Zheng, M.; Kong, F.; Wang, F.; Li, Z.; Bai, T. Numerical simulation of solar assisted ground-source heat pump heating system with latent heat energy storage in severely cold area. *Appl. Therm. Eng.* **2008**, *28*, 1427–1436. [[CrossRef](#)]
53. Qi, Q.; Deng, S.; Jiang, Y. A simulation study on a solar heat pump heating system with seasonal latent heat storage. *Sol. Energy* **2008**, *82*, 669–675. [[CrossRef](#)]
54. Kutlu, C.; Zhang, Y.; Elmer, T.; Su, Y.; Riffat, S. A simulation study on performance improvement of solar assisted heat pump hot water system by novel controllable crystallization of supercooled PCMs. *Renew. Energy* **2020**, *152*, 601–612. [[CrossRef](#)]
55. Döğüşcü, D.K.; Hekimoğlu, G.; Sarı, A. High internal phase emulsion templated-polystyrene/carbon nano fiber/hexadecanol composites phase change materials for thermal management applications. *J. Energy Storage* **2021**, *39*, 102674. [[CrossRef](#)]
56. Cui, Y.; Liu, C.; Hu, S.; Yu, X. The experimental exploration of carbon nanofiber and carbon nanotube additives on thermal behavior of phase change materials. *Sol. Energy Mater. Sol. Cells* **2011**, *95*, 1208–1212. [[CrossRef](#)]
57. Kuziel, A.W.; Dzido, G.; Turczyn, R.; Jędrzyśiak, R.G.; Kolanowska, A.; Tracz, A.; Zięba, W.; Cyganiuk, A.; Terzyk, A.P.; Boncel, S. Ultra-long carbon nanotube-paraffin composites of record thermal conductivity and high phase change enthalpy among paraffin-based heat storage materials. *J. Energy Storage* **2021**, *36*, 102396. [[CrossRef](#)]
58. Tang, Y.; Alva, G.; Huang, X.; Su, D.; Liu, L.; Fang, G. Thermal properties and morphologies of MA–SA eutectics/CNTs as composite PCMs in thermal energy storage. *Energy Build.* **2016**, *127*, 603–610. [[CrossRef](#)]
59. Wang, S.; Cheng, Q.; Gan, Y.; Li, Q.; Liu, C.; Sun, W. Effect of Wax Composition and Shear Force on Wax Aggregation Behavior in Crude Oil: A Molecular Dynamics Simulation Study. *Molecules* **2022**, *27*, 4432. [[CrossRef](#)]
60. Klochko, L.; Noel, J.; Sgreva, N.R.; Leclerc, S.; Metivier, C.; Lacroix, D.; Isaiev, M. Thermophysical properties of n-hexadecane: Combined molecular dynamics and experimental investigations. *Int. Commun. Heat Mass Transf.* **2022**, *137*, 106234. [[CrossRef](#)]
61. Du, Y.; Zhou, T.; Zhao, C.; Ding, Y. Molecular dynamics simulation on thermal enhancement for carbon nano tubes (CNTs) based phase change materials (PCMs). *Int. J. Heat Mass Transf.* **2022**, *182*, 122017. [[CrossRef](#)]

62. Zou, D.; Ma, X.; Liu, X.; Zheng, P.; Hu, Y. Thermal performance enhancement of composite phase change materials (PCM) using graphene and carbon nanotubes as additives for the potential application in lithium-ion power battery. *Int. J. Heat Mass Transf.* **2018**, *120*, 33–41. [[CrossRef](#)]
63. Lin, Y.; Cong, R.; Chen, Y.; Fang, G. Thermal properties and characterization of palmitic acid/nano silicon dioxide/graphene nanoplatelet for thermal energy storage. *Int. J. Energy Res.* **2020**, *44*, 5621–5633. [[CrossRef](#)]
64. Liu, X.; Rao, Z. Experimental study on the thermal performance of graphene and exfoliated graphite sheet for thermal energy storage phase change material. *Thermochim. Acta* **2017**, *647*, 15–21. [[CrossRef](#)]
65. Zhang, M.; Wang, C.; Luo, A.; Liu, Z.; Zhang, X. Molecular dynamics simulation on thermophysics of paraffin/EVA/graphene nanocomposites as phase change materials. *Appl. Therm. Eng.* **2020**, *166*, 114639. [[CrossRef](#)]
66. Huang, Z.; Wang, C.; Zhou, L.; Wu, C. Thermal conductivity enhancement and shape stability of phase-change materials using high-strength 3D graphene skeleton. *Surfaces Interfaces* **2021**, *26*, 101338. [[CrossRef](#)]
67. Atinafu, D.G.; Wang, C.; Dong, W.; Chen, X.; Du, M.; Gao, H.; Wang, G. In-situ derived graphene from solid sodium acetate for enhanced photothermal conversion, thermal conductivity, and energy storage capacity of phase change materials. *Sol. Energy Mater. Sol. Cells* **2020**, *205*, 110269. [[CrossRef](#)]
68. Yang, J.; Qi, G.Q.; Bao, R.Y.; Yi, K.; Li, M.; Peng, L.; Cai, Z.; Yang, M.B.; Wei, D.; Yang, W. Hybridizing graphene aerogel into three-dimensional graphene foam for high-performance composite phase change materials. *Energy Storage Mater.* **2018**, *13*, 88–95. [[CrossRef](#)]
69. Huang, X.; Lin, Y.; Alva, G.; Fang, G. Thermal properties and thermal conductivity enhancement of composite phase change materials using myristyl alcohol/metal foam for solar thermal storage. *Sol. Energy Mater. Sol. Cells* **2017**, *170*, 68–76. [[CrossRef](#)]
70. Zheng, H.; Wang, C. Numerical and experimental studies on the heat transfer performance of copper foam filled with paraffin. *Energies* **2017**, *10*, 902. [[CrossRef](#)]
71. Ferfera, R.S.; Madani, B. Thermal characterization of a heat exchanger equipped with a combined material of phase change material and metallic foams. *Int. J. Heat Mass Transf.* **2020**, *148*, 119162. [[CrossRef](#)]
72. Xiao, Q.; Zhang, M.; Fan, J.; Li, L.; Xu, T.; Yuan, W. Thermal conductivity enhancement of hydrated salt phase change materials employing copper foam as the supporting material. *Sol. Energy Mater. Sol. Cells* **2019**, *199*, 91–98. [[CrossRef](#)]
73. Li, T.; Wu, D.; He, F.; Wang, R. Experimental investigation on copper foam/hydrated salt composite phase change material for thermal energy storage. *Int. J. Heat Mass Transf.* **2017**, *115*, 148–157. [[CrossRef](#)]
74. Wen, R.; Zhu, X.; Yang, C.; Sun, Z.; Zhang, L.; Xu, Y.; Qiao, J.; Wu, X.; Min, X.; Huang, Z. A novel composite phase change material from lauric acid, nano-Cu and attapulgite: Preparation, characterization and thermal conductivity enhancement. *J. Energy Storage* **2022**, *46*, 103921. [[CrossRef](#)]
75. Tang, F.; Cao, L.; Fang, G. Preparation and thermal properties of stearic acid/titanium dioxide composites as shape-stabilized phase change materials for building thermal energy storage. *Energy Build.* **2014**, *80*, 352–357. [[CrossRef](#)]
76. Zhao, B.; Wang, Y.; Wang, C.; Zhu, R.; Sheng, N.; Zhu, C.; Rao, Z. Thermal conductivity enhancement and shape stabilization of phase change thermal storage material reinforced by combustion synthesized porous Al₂O₃. *J. Energy Storage* **2021**, *42*, 103028. [[CrossRef](#)]
77. Li, Q.; Yu, Y.; Liu, Y.; Liu, C.; Lin, L. Thermal properties of the mixed n-octadecane/Cu nanoparticle nanofluids during phase transition: A molecular dynamics study. *Materials* **2017**, *10*, 38. [[CrossRef](#)] [[PubMed](#)]
78. Liu, X.; Adibi, M.; Shahgholi, M.; Tlili, I.; Sajadi, S.M.; Abdollahi, A.; Li, Z.; Karimipour, A. Phase change process in a porous Carbon-Paraffin matrix with different volume fractions of copper oxide Nanoparticles: A molecular dynamics study. *J. Mol. Liq.* **2022**, *366*, 120296. [[CrossRef](#)]
79. Fu, W.; Zou, T.; Liang, X.; Wang, S.; Gao, X.; Zhang, Z.; Fang, Y. Thermal properties and thermal conductivity enhancement of composite phase change material using sodium acetate trihydrate-urea/expanded graphite for radiant floor heating system. *Appl. Therm. Eng.* **2018**, *138*, 618–626. [[CrossRef](#)]
80. Chandel, S.; Agarwal, T. Review of current state of research on energy storage, toxicity, health hazards and commercialization of phase changing materials. *Renew. Sustain. Energy Rev.* **2017**, *67*, 581–596. [[CrossRef](#)]
81. Salunkhe, P.B.; Shembekar, P.S. A review on effect of phase change material encapsulation on the thermal performance of a system. *Renew. Sustain. Energy Rev.* **2012**, *16*, 5603–5616. [[CrossRef](#)]
82. Jacob, R.; Bruno, F. Review on shell materials used in the encapsulation of phase change materials for high temperature thermal energy storage. *Renew. Sustain. Energy Rev.* **2015**, *48*, 79–87. [[CrossRef](#)]
83. Arshad, A.; Jabbar, M.; Yan, Y.; Darkwa, J. The micro-/nano-PCMs for thermal energy storage systems: a state of art review. *Int. J. Energy Res.* **2019**, *43*, 5572–5620. [[CrossRef](#)]
84. Radouane, N. A Comprehensive Review of Composite Phase Change Materials (cPCMs) for Thermal Management Applications, Including Manufacturing Processes, Performance, and Applications. *Energies* **2022**, *15*, 8271. [[CrossRef](#)]
85. Liu, C.; Wang, C.; Li, Y.; Rao, Z. Preparation and characterization of sodium thiosulfate pentahydrate/silica microencapsulated phase change material for thermal energy storage. *Rsc Adv.* **2017**, *7*, 7238–7249. [[CrossRef](#)]
86. Fang, Y.; Huang, L.; Liang, X.; Wang, S.; Wei, H.; Gao, X.; Zhang, Z. Facilitated synthesis and thermal performances of novel SiO₂ coating Na₂HPO₄·7H₂O microcapsule as phase change material for thermal energy storage. *Sol. Energy Mater. Sol. Cells* **2020**, *206*, 110257. [[CrossRef](#)]

87. Liu, Z.; Chen, Z.; Yu, F. Preparation and characterization of microencapsulated phase change materials containing inorganic hydrated salt with silica shell for thermal energy storage. *Sol. Energy Mater. Sol. Cells* **2019**, *200*, 110004. [[CrossRef](#)]
88. Fu, W.; Zou, T.; Liang, X.; Wang, S.; Gao, X.; Zhang, Z.; Fang, Y. Characterization and thermal performance of microencapsulated sodium thiosulfate pentahydrate as phase change material for thermal energy storage. *Sol. Energy Mater. Sol. Cells* **2019**, *193*, 149–156. [[CrossRef](#)]
89. Sami, S.; Sadrameli, S.; Etesami, N. Thermal properties optimization of microencapsulated a renewable and non-toxic phase change material with a polystyrene shell for thermal energy storage systems. *Appl. Therm. Eng.* **2018**, *130*, 1416–1424. [[CrossRef](#)]
90. Zhang, N.; Yuan, Y. Synthesis and thermal properties of nanoencapsulation of paraffin as phase change material for latent heat thermal energy storage. *Energy Built Environ.* **2020**, *1*, 410–416. [[CrossRef](#)]
91. Chen, W.; Liang, X.; Wang, S.; Gao, X.; Zhang, Z.; Fang, Y. Polyurethane macro-encapsulation for $\text{CH}_3\text{COONa} \cdot 3\text{H}_2\text{O} \cdot \text{Na}_2\text{S}_2\text{O}_3 \cdot 5\text{H}_2\text{O}$ /Melamine sponge to fabricate form-stable composite phase change material. *Chem. Eng. J.* **2021**, *410*, 128308. [[CrossRef](#)]
92. Rao, Z.; Wang, S.; Peng, F. Self diffusion and heat capacity of n-alkanes based phase change materials: A molecular dynamics study. *Int. J. Heat Mass Transf.* **2013**, *64*, 581–589. [[CrossRef](#)]
93. Rao, Z.; Wang, S.; Peng, F. Molecular dynamics simulations of nano-encapsulated and nanoparticle-enhanced thermal energy storage phase change materials. *Int. J. Heat Mass Transf.* **2013**, *66*, 575–584. [[CrossRef](#)]
94. Singh, P.; Sharma, R.; Ansu, A.; Goyal, R.; Sari, A.; Tyagi, V. A comprehensive review on development of eutectic organic phase change materials and their composites for low and medium range thermal energy storage applications. *Sol. Energy Mater. Sol. Cells* **2021**, *223*, 110955. [[CrossRef](#)]
95. Da Cunha, J.P.; Eames, P. Thermal energy storage for low and medium temperature applications using phase change materials—a review. *Appl. Energy* **2016**, *177*, 227–238. [[CrossRef](#)]

Disclaimer/Publisher's Note: The statements, opinions and data contained in all publications are solely those of the individual author(s) and contributor(s) and not of MDPI and/or the editor(s). MDPI and/or the editor(s) disclaim responsibility for any injury to people or property resulting from any ideas, methods, instructions or products referred to in the content.